Gain amplification and lasing properties of individual organic nanofibers

F. Quochi,[a)] F. Cordella, A. Mura, and G. Bongiovanni
Dipartimento di Fisica, Università di Cagliari, I-09042 Monserrato (CA), Italy

F. Balzer
Institut für Physik/ASP, Humboldt-Universität zu Berlin, Newtonstrasse 15, D-12489 Berlin, Germany

H.-G. Rubahn
Fysisk Institut, Syddansk Universitet, Campusvej 55, DK-5230 Odense M, Denmark

We study gain and lasing processes in individual self-assembled organic nanofibers grown on mica substrates. The gain-induced response of the nanofibers is found to depend sensitively on the fiber structure. In homogeneous fibers where no coherent optical feedback is present, high net optical gain (of up to 10^3 cm^{-1}) results in spectral narrowing at the material gain peaks. In the case of strong optical feedback, which occurs in long nanofibers with randomly distributed scattering centers, gain is in turn responsible for low-threshold coherent random laser action. © *2006 American Institute of Physics.* [DOI: 10.1063/1.2167397]

The observation of amplified spontaneous emission (ASE) in π-conjugated molecules and polymers in the solid state has dramatically increased the potential of semiconducting organics for optoelectronic applications.[1] Within the polymer film approach, suitable modulation of the film thickness (e.g., via periodic two-dimensional patterning) has been used to attain low-threshold laser action on well-controlled cavity modes.[2] Molecular epitaxy has in turn shown the ease of fabrication, by self-assembly mechanisms, of morphologically diverse nanoaggregates, in which strong optical confinement can be realized. Among this class of molecular systems lie organic nanofibers.[3] In these needle-shaped systems, two-dimensional optical confinement enables single-mode waveguiding of visible light[4,5] and enhancement of nonlinear optical effects.[6] The recent observation of low-threshold coherent emission from thin films of close-packed *para*-sexiphenyl (*p*-6P) nanofibers on mica substrates has been ascribed to random laser action taking place in closed-loop optical cavities realized within the tight fiber crossconnect.[7] Further investigations have then elucidated the one-dimensional nature of the distributed optical feedback taking place in isolated nanofibers.[8]

In this letter, we study both gain amplification and lasing processes in *singly selected p*-6P nanofibers grown on mica. A deep change in the nonlinear optical response from coherent random lasing to featureless spectral narrowing caused by ASE is observed when removing the optical feedback produced by reflection centers randomly distributed across the fibers.

The nanofiber films are grown on freshly cleaved muscovite mica by vacuum sublimation. Deposition occurs at a typical rate of 0.2 Å/s under a dynamic vacuum of $\approx10^{-7}$ mbar, at a substrate temperature around 420 K. An inverted microscope is used to image the fluorescence of the nanofiber films excited by a cw arc source in the 330–380 nm spectral band. For gain amplification and lasing measurements, we use ultrafast photopumping at 390 nm (150 fs pulses @ 1 kHz repetition rate). Typical excitation

spots are 180 μm in diameter. Time integrated fluorescence/lasing measurements are made in transmission geometry by detecting the emission scattered out of the substrate plane. A high-sensitivity microspectrographic system is used, which enables us to take micrographs with a spatial resolution of 2 μm, or, alternatively, space-wavelength spectrograms of single nanofibers with a spatial resolution of 2 μm and a spectral resolution of 0.2 nm.

Figure 1 displays a fluorescence micrograph of isolated nanofibers having lengths of up to several hundred micrometers (not shown) and ranging typically from 200 to 400 nm in base width, thereby enabling waveguiding of visible light. Bright spots of scattered fluorescence correspond to narrow ($\sim$100 nm wide) breaks distributed along the needles, as demonstrated by correlated optical and topographic measurements. These naturally occurring breaks have been inferred to be responsible for recurrent light scattering within the needles, so leading to one-dimensional random lasing in individual *p*-6P nanofibers.[8]

Nonlinear optical emission from the nanofibers is observed using ultrafast excitation with fluences larger than 10 μJ/cm^2 per pulse. Long nanofibers ($>$50–100 μm), which are in fact segmented into many sections by breaks,
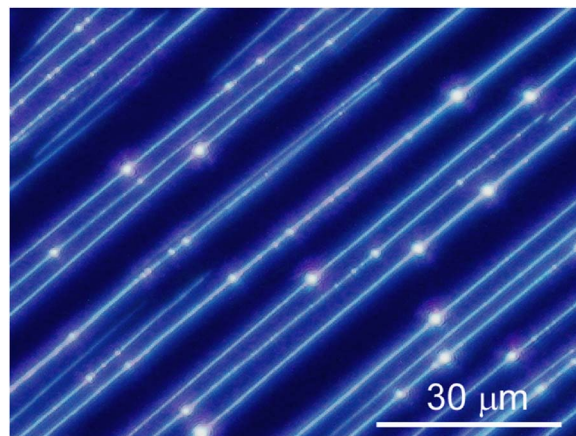
FIG. 1. (Color online) Fluorescence micrograph of *para*-sexiphenyl nanofibers deposited on (001)-oriented muscovite mica.

[a)]Author to whom correspondence should be addressed; electronic mail: francesco.quochi@dsf.unica.it
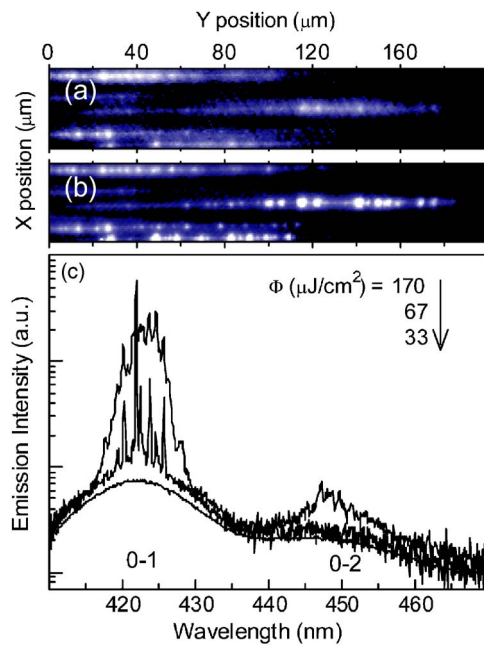
FIG. 2. (Color online) Time integrated optical emission micrographs of nanofibers excited by ultrafast pulses, for a pump fluence of 33 (a) and 170 $\mu J/cm^2$ per pulse (b). Panel (c) Time integrated emission spectra of the nanofiber placed at the center of the X position range in panels (a) and (b), for different values of the excitation fluence. The spectra are spatially integrated over the nanofiber region (from $Y \approx 10$ μm to $Y \approx 185$ μm).

FIG. 3. (Color online) Time integrated optical emission micrographs of a nanofiber excited by ultrafast pulses, for a pump fluence of 75 (a) and 370 $\mu J/cm^2$ per pulse (b). Panel (c) Time integrated emission spectra of the same nanofiber for different values of the excitation fluence. The spectra are spatially integrated over the nanofiber region (from $Y \approx 88$ μm to $Y \approx 128$ μm).

exhibit nonlinear emission spectra typical for coherent random lasing, with resolution-limited spikes that emerge from the spontaneous emission spectrum as soon as a threshold value in pump fluence is reached[9] [Fig. 2(c)]. In such nanofibers the spatial distribution of the emission intensity scattered into out-of-plane directions towards collecting optics is highly inhomogeneous. Enhancement of emission scattering is observed at the fiber break locations already below oscillation threshold [Fig. 2(a)], although the bright spot contrast increases dramatically above threshold due to the coherent nature of the emitted light [Fig. 2(b)].

Since efficient recurrent scattering in the needle axis' direction realizes long closed-loop paths for light amplification, oscillation on random modes starts at low pump fluences. Low-threshold laser action including random lasing is suitable for application purposes; however, its phenomenology makes it difficult to retrieve information on the underlying waveguide ASE process, which relates more closely to the intrinsic photonic response of the nanofibers. In the following, we will show that it is possible to inhibit coherent oscillation and single out the process of waveguide ASE by removing the source of optical feedback in the fibers. ASE without coherent feedback should be observed in nanofibers without breaks.

Breakless fibers are identified by checking for the absence of intense scattering spots in the optical emission patterns. Figure 3 displays the results obtained in such a nanofiber. Micrographs taken at low pump fluences [where only spontaneous emission is detected, Fig. 3(a)] show that the fiber emission is rather homogenous. When the pump fluence is raised above a threshold value [Fig. 3(b)], strong increase in scattered intensity is revealed at the fiber end regions, suggesting the occurrence of light amplification in the fiber waveguide with outcoupling at the fiber tips. As expected in the case of ASE, the emission spectra exhibit line narrowing
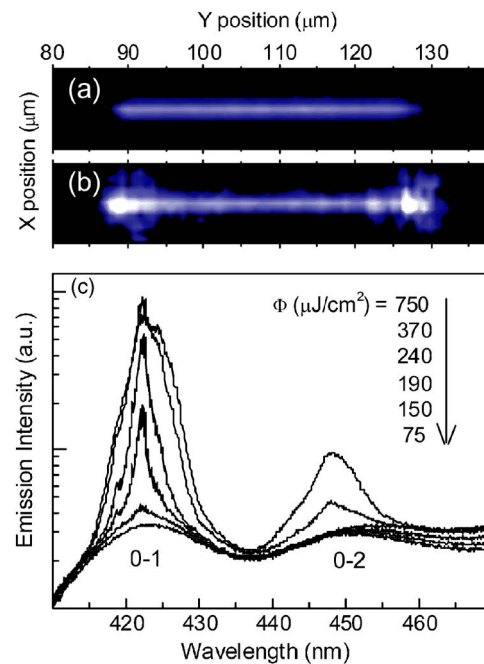
for increasing pump fluence [Fig. 3(c)]. Spectral narrowing is detected at both the 0–1 and 0–2 vibronic peaks of p-6P. Gain saturation effects are also observed at high fluences (>350 $\mu J/cm^2$) on the 0–1 band. The lack of sharp spectral features implies the absence of coherent feedback in the fiber structure,[10] from which we infer that the fiber tips are not characterized by very well defined facets. In order to retrieve optical gain, breakless fibers can thus be modeled as optical amplifiers without feedback.

Figure 4(a) shows the scattered emission intensity profiles extracted from the micrographs reported in Figs. 3(a) and 3(b). While the emission profile is almost constant across the whole nanofiber at low pump fluences, above the onset of spectral narrowing the scattered intensity is position dependent and increases as the position approaches the end tips.
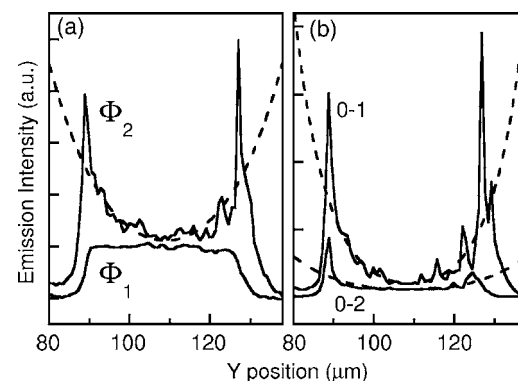
FIG. 4. Panel (a) Time and spectrally integrated spatial profiles of the emission intensity of the nanofiber shown in Fig. 3, for two pump fluences: Φ_1 =75 $\mu J/cm^2$ and Φ_2=370 $\mu J/cm^2$ per pulse. Panel (b) Intensity profiles spectrally resolved for the 0–1 and 0–2 vibronic bands, for a pump fluence of 750 $\mu J/cm^2$ per pulse. The dashed lines in both panels are fits to the data. The fit curves are extended outside the nanofiber region for better visibility.

This is consistent with the ASE process as inferred from spectral narrowing. From the emission spectrograms, we then generate two independent emission spatial profiles for the 0–1 and 0–2 emission bands [shown in Fig. 4(b)].

To estimate the amount of net gain in our nanofiber-based waveguide, we consider that ASE yields an output intensity $I(L) \sim [\exp(gL) - 1]/g$,[1] where L is the length of the amplifying region and g is the net (modal) gain coefficient. Inside the nanofiber (of length L), the total intensity of the amplified light at a distance d from a fiber tip will thus be $I_T(d) = I(d) + I(L-d)$. Assuming that the scattering efficiency is independent of position over the whole nanofiber length,[11] the same function $I_T(d)$ can be used for curve fitting to the measured intensity spatial profiles, using g as a free parameter. Fit curves for $L = 40$ μm are shown as the dashed lines in Figs. 4(a) and 4(b).[12] For the profiles relating to the 0–1 and 0–2 bands, best fitting yields the net gain values $g_{0-1} = (1250 \pm 100)$ cm^{-1} and $g_{0-2} = (750 \pm 100)$ cm^{-1} at the (highest) pump fluence of 750 μJ/cm^2 per pulse. ASE kicks in when the net gain value is comparable to the inverse fiber length ($g \sim L^{-1}$); that explains why in short nanofibers the ASE threshold fluence is rather high.

In the limit of linear absorption of the pump energy, the excitation density (N) created by each pulse (at the highest pump fluence) is estimated to be $\sim 10^{20}$ cm^{-3}.[7] Further neglecting population/gain time relaxation, the stimulated emission cross section (σ_{SE}) of p-6P can be estimated from the relation $g = \Gamma g_{mat} - \alpha$,[13] where $g_{mat} = \sigma_{SE} N$ is the material gain coefficient, Γ is the confinement factor of the optical intensity inside the nanofiber, and α is the total propagation loss.[14] Based on Maxwell's equations solved for dielectric waveguides on a substrate support,[4] the optical confinement factor in typical p-6P nanofibers deposited on mica is estimated to be $\sim 1\%$, while previous optical waveguiding experiments in singly selected organic nanofibers yielded $\alpha \sim 100 - 300$ cm^{-1}.[4] Using $g = 1250$ cm^{-1}, $\Gamma = 0.01$, $N = 10^{20}$ cm^{-3} and $\alpha = 300$ cm^{-1}, we obtain $\sigma_{SE} \approx 1.5 \times 10^{-15}$ cm^2. Our estimate is in fact supported by recent experimental reports of σ_{SE} values as large as 10^{-15} cm^2 in films of π-conjugated polymers[15] (6×10^{-16} cm^2 in polycrystalline films of oligothiophene derivatives).[16] The high gain and lasing performance of p-6P nanofibers is expected to motivate further investigations of the population/gain dynamics and photonic properties of self-assembled organic nanoaggregates.

In conclusion, we studied the nonlinear optical response of individual p-6P organic nanofibers. Depending on the nanofiber structure, either low-threshold coherent random lasing or ASE with waveguide net gain values of $\sim 10^3$ cm^{-1} are detected at the p-6P emission peaks in the blue. Therefore, the capability of finely controlling and modulating the nanofiber self-assembly process could enable various applications of organic nanofibers in the field of subwavelength photonics in the future.

[1] For a review, see, e.g., M. D. McGehee and A. J. Heeger, Adv. Mater. (Weinheim, Ger.) **12**, 1655 (2000), and references therein.

[2] G. Heliotis, R. Xia, G. A. Turnbull, P. Andrew, W. L. Barnes, I. D. W. Samuel, and D. D. C. Bradley, Adv. Funct. Mater. **14**, 91 (2004).

[3] H. Yanagi and T. Morikawa, Appl. Phys. Lett. **75**, 187 (1999); A. Andreev, G. Matt, C. J. Brabec, H. Sitter, D. Badt, H. Seyringer, and N. S. Sariciftci, Adv. Mater. (Weinheim, Ger.) **12**, 629 (2000); F. Balzer and H.-G. Rubahn, Appl. Phys. Lett. **79**, 3860 (2001).

[4] F. Balzer, V. G. Bordo, A. C. Simonsen, and H.-G. Rubahn, Phys. Rev. B **67**, 115408 (2003); V. S. Volkov, S. I. Bozhevolnyi, V. G. Bordo, and H.-G. Rubahn, J. Microsc. **215**, 241 (2004).

[5] K. Takazawa, Y. Kitahama, Y. Kimura, and G. Kido, Nano Lett. **5**, 1293 (2005).

[6] H. Yanagi and A. Yoshiki, Appl. Phys. Lett. **84**, 4783 (2004).

[7] F. Quochi, F. Cordella, R. Orrù, J. E. Communal, P. Verzeroli, A. Mura, G. Bongiovanni, A. Andreev, H. Sitter, and N. S. Sariciftci, Appl. Phys. Lett. **84**, 4454 (2004).

[8] F. Quochi, F. Cordella, A. Mura, G. Bongiovanni, F. Balzer, and H.-G. Rubahn, J. Phys. Chem. B **109**, 21690 (2005).

[9] H. Cao, J. Y. Xu, S.-H. Chang, and S. T. Ho, Phys. Rev. E **61**, 1985 (2000).

[10] Weak interference fringes spaced by ~ 0.4 nm are revealed on the 0–1 ASE band, which might originate from reflections at the backsurface of the substrate.

[11] This assumption is supported by the uniformity of the intensity profiles taken at pump fluences below the ASE onset [Fig. 4(a)].

[12] Note that the tip regions are excluded from the fitting procedure since the scattering efficiency is strongly enhanced at the fiber tips.

[13] L. Wu, W. Tian, and F. Gao, Semicond. Sci. Technol. **19**, 1149 (2004).

[14] Propagation optical losses are attributed to material self-absorption and scattering by nanofiber surface roughness.

[15] S. V. Frolov, M. Ozaki, W. Gellermann, K. Yoshino, and Z. V. Vardeny, Phys. Rev. Lett. **78**, 729 (1997).

[16] D. Pisignano, M. Anni, G. Gigli, R. Cingolani, M. Zavelani-Rossi, G. Lanzani, G. Barbarella, and L. Favaretto, Appl. Phys. Lett. **81**, 3534 (2002).